JIDR Journal of Intellectual Disability Research
Published on behalf of mencap and in association with IASSID

Journal of Intellectual Disability Research doi: 10.1111/j.1365-2788.2011.01490.x

VOLUME 56 PART 9 pp 879–894 SEPTEMBER 2012

Williams syndrome: a relationship between genetics, brain morphology and behaviour

C. Fahim,[1,4] U. Yoon,[2] N. H. Nashaat,[3] A. K. Khalil,[4] M. El-Belbesy,[5] A. Mancini-Marie,[6] A. C. Evans[7] & N. Meguid[3]

1 *Institute of Psychology, Faculty of Social Sciences and Politics, University of Lausanne, Lausanne, Switzerland*
2 *Department of Biomedical Engineering, Catholic University of Daegu, Hayang-eup, Gyeongsan, South Korea*
3 *Department of Research on Children with Special Needs, Medical Genetics Division, The National Research Centre, Cairo, Egypt*
4 *Department of Cytogenetics, Molecular Genetics Division, The National Research Centre, Cairo, Egypt*
5 *Medical Research Institute, Alexandria University, Alexandria, Egypt*
6 *Department of Psychiatry, Hôpitaux Universitaires de Genève HUG, University of Geneva, Geneva, Switzerland*
7 *McConnell Brain Imaging Centre, the Montreal Neurological Institute and the Department of Neurology and Neurosurgery, Faculty of Medicine, McGill University, Montreal, Québec, Canada*

Abstract

Background Genetically Williams syndrome (WS) promises to provide essential insight into the pathophysiology of cortical development because its ~28 deleted genes are crucial for cortical neuronal migration and maturation. Phenotypically, WS is one of the most puzzling childhood neurodevelopmental disorders affecting most intellectual deficiencies (i.e. low-moderate intelligence quotient, visuospatial deficits) yet relatively preserving what is uniquely human (i.e. language and social-emotional cognition). Therefore, WS provides a privileged setting for investigating the relationship between genes, brain and the consequent complex human behaviour.

Methods We used *in vivo* anatomical magnetic resonance imaging analysing cortical surface-based morphometry, (i.e. surface area ϒSA/, cortical volume ϒCV/, cortical thickness ϒCth/, gyrification index ϒGI/) and cortical complexity ϒCC/, which is of particular relevance to the WS genotype–phenotype relationship in 22 children (2.27–14.6 years) to compare whole hemisphere and lobar surface-based morphometry between WS ($n = 10$) and gender/age matched normal controls healthy controls ($n = 12$).

Results Compared to healthy controls, WS children had a (1) relatively preserved Cth; (2) significantly reduced SA and CV; (3) significantly increased GI mostly in the parietal lobe; and (4) decreased CC specifically in the frontal and parietal lobes.

Conclusion Our findings are then discussed with reference to the Rakic radial-unit hypothesis of cortical development, arguing that WS gene deletions may spare Cth yet affecting the number of founder cells/columns/radial units, hence decreasing the SA and CV. In essence, cortical brain structure in WS may be shaped by gene-dosage abnormalities.

Keywords cortical surface, cortical volume, gyrification, radial-unit hypothesis, structural magnetic resonance imaging, Williams syndrome

Introduction

Williams syndrome (WS) children are highly sociable (Morris *et al.* 1990), approachable, less

Correspondence: Dr Cherine Fahim, Université de Lausanne, Institut de Psychologie, Faculté de Sciences Sociales et Politiques, Lausanne 1015 Vaud, Suisse (e-mail: cherine.fahim@unil.ch).

reserved towards strangers (Tomc *et al.* 1990), extremely friendly (Gosch & Pankau 1997), loquacious (Plissart *et al.* 1994), displaying high musical abilities (Lenhoff *et al.* 2001), intelligence quotient (IQ) varying from 20 to 106 (Ewart *et al.* 1993) with a remarkable deficit in visuospatial construction (Klein & Mervis 1999), attentional and anxiety problems (Cherniske *et al.* 2004). This is how most clinical neuroscientists characterise WS, which genetically results from a deletion of the Williams–Beuren syndrome chromosome 7q11.23 region, spanning 1.5 million to 1.8 million base pairs and containing 26 to 28 genes (reviewed in Pober 2010). Of particular relevance to the present paper, the WS 26 to 28 gene deletions include genes that are crucial for neuronal migration, maturation and the consequent cortical organisation. In this context, WS provides a privileged setting for investigating how such a unique behavioural phenotype shapes the brain? Or should we ask how such a genetic/neuroanatomic profile shapes behaviour in WS?

Five of the genes involved in WS, *FZD3*, *BCL7B* (*WS-bTRP*, *WS-bHLH*), *STX1A*, *LIMK1* and *CYLN2*, are known to have neuronal expression and thus are of interest as candidates for the WS behavioural phenotype (Morris & Mervis 2000). These genes are on a region that is bordered by repeats, leading to the hypothesis that WS is caused by illegitimate homologous recombination at the repeats during meiosis (Hoogenraad *et al.* 2002). The *FZD3* is involved in early development of a large domain of the central nervous system encompassing much of the midbrain and rostral metencephalon (Wang *et al.* 1997). *LIM-kinase 1* hemizygosity has been implicated as a contributing factor to impaired visuospatial constructive cognition in WS (Frangiskakis *et al.* 1996). In 1998, Meng and colleagues (Meng *et al.* 1998) stated that hemizygous deletion of one or more of the *BCL7B and its related genes WS-bTRP*, *WS-bHLH* may contribute to developmental defects in WS. Of particular relevance to cortical surface area (SA) decrease in WS, a human brain malformation, Miller–Dieker lissencephaly, manifested by a smooth cerebral surface and abnormal neuronal migration, is caused by hemizygous deletion implicating the WS-bTRP. Notably, WS-bHLH transcription factors are important regulators of neurogenesis, myogenesis, cell proliferation and differentiation, and cell lineage determination. In this vein, quantitative cytoarchitectonic studies demonstrated several cytoarchitectonical anomalies, which included a *reduction in columnar organisation* throughout the cortex, *abnormal neuronal orientation* and a *generalised increase in cell packing density* (Galaburda *et al.* 1994). Neuroimaging studies concluded that some of the grey matter in the frontal and temporal limbic structures is relatively preserved in WS. However, the authors reported more severe decrease in volume in posterior cortical regions. Interestingly, such topographic distribution of severity of abnormalities is in agreement with the WS behavioural phenotype, specifically regarding visuospatial impairment and parieto-occipital volumes (Jernigan *et al.* 1993). Following these reports, anatomical magnetic resonance imaging had a great impact on deciphering the WS neuroendophenotype, for example, (1) Reiss and colleagues showed decreased overall brain and cerebral volumes, relative preservation of cerebellar and superior temporal gyrus volumes, and disproportionate volume reduction of the brainstem, parietal and occipital lobes (Reiss *et al.* 2000); (2) Galaburda and colleagues (Galaburda *et al.* 2001) found that the dorsal central sulcus was less likely to reach the interhemispheric fissure bilaterally. The authors concluded that early neurodevelopmental problems affect the development of the dorsal forebrain and are probably related to the deficits in visuospatial ability and behavioural timing often observed in WS; (3) decreased parieto-occipital lobe volumes relative to frontal regions (Schmitt *et al.* 2001); (4) structural-functional alterations in the brain visuospatial construction (Meyer-Lindenberg *et al.* 2004); (5) increased cortical thickness (Cth) (Thompson *et al.* 2005); bilateral reductions in sulcal depth in the intraparietal/occipitoparietal sulcus (Kippenhan *et al.* 2005); (6) increased gyrification (Gaser *et al.* 2006); and (7) alteration in white matter fibre directionality, deviation in posterior fibre tract course, and reduced lateralisation of fibre coherence (Marenco *et al.* 2007). Although these seminal studies agree on the presence of cortical abnormalities in WS, each took a small piece of the WS cortical abnormalities puzzle and analysed it without actually attempting to assemble the whole puzzle. Here, we (1) investigate the first comprehensive three-dimensional (3D) maps of cortical patterns, including Cth, SA, cortical volume (CV),

gyrification index (GI) and cortical complexity (CC); and (2) correlate brain morphology and neuropsychological measures during early childhood in WS. Based on all of the seminal literature cited above, à priori we expected a relationship between a deletion of the WS chromosome 7q11.23 region, brain morphology (i.e. Cth, SA, CV, GI and CC) and neuropsychological tests. Specifically we advanced the hypothesis that total and regional SA and lobar volumes will be reduced in WS relative to children with typical development, which will correlate with neuropsychological measures.

Methods

Participants

Children with WS were recruited from the National Research Centre within the Swiss Egyptian Neurodevelopmental Study initiated by the Egyptian Neuroimaging Neurodevelopmental Genetics Initiative Network. They were genetically tested with fluorescence in situ hybridisation to verify the typical hemideletions in the WS critical area of chromosome 7q11.23 (Morris & Mervis 2000). Healthy controls (HC) free of neuropsychiatric or medical disorders that could affect brain structure and function were matched individually by age, gender and socio-economical class to the WS children. HC were also recruited in Egypt. All participants underwent thorough consent and assent procedures before commencing study procedures according to the declaration of Helsinki. Parent or legal guardian consent was obtained for all individuals. The study was approved by the National Research Centre institutional review board according to the ethical guidelines of the Medical Service Unit. All participants were pre-screened for magnetic resonance imaging compatibility before commencing the neuroimaging procedures. The sample was composed of Egyptian participants. Of note, Egypt the geographic location of Egypt, at the interface between Southern Europe, the Middle East and North Africa is of particular interest. The Y-chromosome gene pool in the modern Egyptian population reflects a mixture of European, Middle Eastern and African characteristics, highlighting the importance of ancient and recent migration waves, followed by gene flow, in the region (Manni *et al.* 2002). In this vein, Egypt allows informative cases so that meaningful conclusions can be drawn. Characteristics of participants are illustrated in Table 1.

Genetic and clinical assessments

Clinical diagnostic criteria ('American Academy of Pediatrics 2001: Health care supervision for children with Williams syndrome'; Preus 1984), in addition to the fluorescence in situ hybridisation involving *ELN*-specific probes were conducted to confirm the WS diagnosis. Clinical diagnosis was based on a distinctive facial appearance (a broad

Table 1 Characteristics of participants

	Mean ± SD		ANOVA	
	WS	HC	*F*	*P*
Age	8.02 ± 4.54	9.00 ± 3.86	0.30	n.s
Language age	5.01 ± 2.76	7.04 ± 2.24	3.60	n.s
Social age	4.71 ± 2.61	8.87 ± 3.73	8.83	0.008
Vineland Social Maturity Scale	61.40 ± 18.25	98.83 ± 10.53	36.22	0.0001
Snijders-Oomen Nonverbal Intelligence	61.70 ± 17.15	110.00 ± 14.01	52.95	0.0001
Spatial tests (mosaics and patterns)	19.86 ± 2.61	28.00 ± 3.84	23.00	0.0001
Memory (immediate memory)	17.86 ± 4.63	33.56 ± 7.50	23.46	0.0001
Concrete reasoning (puzzles and situations)	16.14 ± 3.39	28.56 ± 5.25	29.38	0.0001
Abstract reasoning (categories and analogies)	17.43 ± 4.24	26.00 ± 2.70	24.44	0.0001

ANOVA, analysis of variance; HC, healthy controls; n.s, not significant; WS, Williams syndrome.

forehead, bitemporal narrowing, low nasal root, periorbital fullness, stellate/lacy iris pattern, strabismus, bulbous nasal tip, malar flattening, long philtrum, full lips, wide mouth, full cheeks, dental malocclusion with small widely spaced teeth, small jaw and prominent earlobes), hypercalcemia plus persistent growth failure, heart murmur, hypertension, supravalvular aortic stenosis (narrowing of the ascending aorta above the aortic valve, involving the sinotubular junction), hypersociability, growth retardation, global cognitive impairment. Neurologic abnormalities in WS included hypotonia, hyperreflexia and evidence of cerebellar dysfunction. Molecular analysis confirmed the presence of a single *ELN* allele only rather than two alleles.

Cognitive assessment

All participants passed the Snijders-Oomen Nonverbal Intelligence (SON) Tests, which make a broad assessment of a spectrum of intelligence functions possible without being dependent upon language skills (Snijders & Snijders-Oomen 1976). Four types of subtests were assessed by an experienced paediatric neurologist and phonologist (N. N.): abstract reasoning tests, concrete reasoning tests, spatial tests and memory tests. Abstract reasoning tests (categories and analogies) depend on relations between concepts that are abstract, namely, not bound to time or space. A principle for ordering must be derived from the test materials that have to be applied to new materials. Concrete reasoning tests (puzzles and situations) refer to persons or objects that are bound together by space and time. The accent can be placed on either the spatial or the time dimension, this leads to different types of tests. Spatial tests (mosaics and patterns) resemble concrete reasoning tests in that by both a relationship must be seen within a spatial whole. In concrete reasoning tests the emphasis lies on conceiving meaningful relations between parts of a picture, in spatial tests on form relations between parts of a figure. Memory tests consisted for example of the following: the child is instructed to memorise where the experimenter located a toy in a doll's house (eight items). The instructions to the test can be given verbally or in a nonverbal way by gestures or by a combination of both. An important aspect of the instructions is demonstration by the examiner. Care has been taken not to give extra information in the verbal instruction by naming objects or concepts. This flexibility in the way the instructions are given allows for a natural and stimulating contact. The communication can be adapted to the normal ways of interacting with a particular child. Another important aspect of administering the test is that feedback is given after each item. This feedback also allows for a more natural interaction between examiner and the child and it gives the child a better understanding of the requirements of the task in case the instructions have not been fully understood. Scores on the SON were found to correlate significantly ($r = 0.87$ and $r = 0.64$) with Wechsler Preschool and Primary Scale of Intelligence and the Stanford–Binet respectively (Harris 1982; Moore *et al.* 1998). Notably, four features make the SON a particularly useful tool for assessing preschoolers who otherwise would be difficult to test: (1) it is interesting and appealing to young children; (2) neither receptive nor expressive language is necessary for response; (3) none of the tasks are timed; and (4) the examiner is permitted to help a child who is not succeeding, so that the child does not become discouraged and uncooperative (Harris 1982). Characteristics of participants are illustrated in Table 1.

Magnetic resonance imaging acquisition

In preparation for imaging, all participants received moderate sedation (combination of pentobarbital sodium and fentanyl citrate as per hospital sedation protocol) administered by a nurse and under the supervision of a paediatric anaesthesiologist. A more detailed description appears elsewhere (Ross *et al.* 2005). T1 mprage sequence (1.5T Philips Intera magnetic resonance imaging) was acquired (scan time 8 min, 6 s; pixel 0.98 × 0.98 mm). TR = 9.7 ms; TE = 4 ms; TI = 300 ms; TD = 0 ms using a 12 degrees flip angle. Number of slabs = 1 fixed; slab thickness = 160 mm; slice thickness = 0.98 mm; number of partitions = 164; 3D-OS = 0%; matrix 266*256. Images were then transferred through a secure connection from Egypt to the Montreal Neurological Institute (MNI) in Canada.

Magnetic resonance imaging analysis

Brain volume analysis was done using the fully automated Civet pipeline (Chung *et al.* 2005; Evans 2006; Im *et al.* 2008a,b, 2010; Kim *et al.* 2005; Lerch & Evans 2005; Lee *et al.* 2006; O. Lyttelton *et al.* 2007, 2009; O. C. Sled *et al.* 1998; Zijdenbos *et al.* 2002; Yoon *et al.* 2009). Images were processed using the standard MNI anatomical pipeline. The native magnetic resonance images were normalised into a standardised stereotaxic space using a linear transformation and corrected for intensity non-uniformity (Collins *et al.* 1994, 1995; Sled *et al.* 1998). The registered and corrected volumes were classified into white matter, grey matter, cerebrospinal fluid and background using an advanced neural-net classifier (Zijdenbos *et al.* 2002). The hemispheric surfaces of the inner and outer cortex, which consisted of 40 962 vertices, were automatically extracted using the Constrained Laplacian-Based Automated Segmentation with Proximities algorithm (Kim *et al.* 2005).

Cortical volume

Extracted inner and outer cortical surfaces in native space were masked to original images. We isolated the voxels of the cerebral cortex that were located between two surfaces. The CV was calculated by measuring the volume of the voxels in the whole cortex and in each lobar region.

Cortical surface area

We measured cortical SA, which has been used to suggest an overall degree of folding (Wiegand *et al.* 2005; Luders *et al.* 2006a,b; Thompson *et al.* 2006). The middle cortical surface lies at the geometric centre between the inner and outer cortical surfaces. It provides a relatively unbiased representation of sulcal versus gyral regions. In contrast, the inner cortical surface model overrepresents sulcal regions, and the outer cortical surface model overrepresents gyral regions (Van Essen 2005). We used the middle cortical surface and calculated the SA in the whole cortex and each lobar region, which was the straightforward sum of the areas of the triangles making up the surface model.

Cortical thickness

The inner and outer surfaces had the same number of vertices, and there was a close correspondence between the counterpart vertices of the inner and outer cortical surfaces. The Cth was defined as the Euclidean distance between these linked vertices (Lerch & Evans 2005). We measured the averaged value of the thickness in the whole cortex and each lobar region.

Gyrification index measurement and cortical complexity

An intermediate cortical surface, half-way between the inner and outer Constrained Laplacian-Based Automated Segmentation with Proximities surfaces, was used for measuring the surface morphometrics as it represents a relatively unbiased representation of both sulcal and gyral regions (Van Essen 1997, 2005). The cortical area was calculated in the whole hemisphere and each lobar region by summing the Voronoi area based on geodesic distances over the folded topology of the surface. The middle cortical surface was divided into the sulcal and gyral regions by thresholding the depth map, that is, 3D Euclidean distance from each vertex to the nearest voxel on the convex hull volume (Im *et al.* 2008a, 2010). The threshold of the depth map was determined from the fact that the human cerebral cortex is a highly folded sheet with 60–70% of its SA buried within folds (Zilles *et al.* 1988; Van Essen 1997). The mean GI was defined as the ratio between the total SA and the superficially exposed SA such as the gyral regions in each hemisphere and lobe (Zilles *et al.* 1988).

Statistical methods and analysis

We examined how Cth, SA, CV, GI and CC varied between WS and HC across the whole hemisphere and the four lobes – frontal, parietal, temporal and occipital. The effect of group (WS vs. HC) was examined for the whole hemisphere and the left and right lobes separately. We complemented lobar analyses by an assessment of the effect of group (WS vs. HC) at each of approximately 45 000 points (vertices) on each hemisphere. We used SPSS 17.0 linear regression within Cth, SA, CV, GI and CC for each hemisphere to compare for example,

how Cth is associated with cortical depth and how SA is associated with CV and GI. Furthermore, multiple regression analyses were performed between brain morphology measures and neuropsychological scores. All statistical thresholds were determined by application of the false discovery rate technique (Genovese *et al.* 2002). *P*-values are corrected for multiple thresholds.

Results

Table 1 summarises age, language age, social age, Vineland Social Maturity Scale (VSMS), SON, spatial tests (mosaics and patterns), memory (immediate memory), concrete reasoning (puzzles and situations) and abstract reasoning (categories and analogies). Results from the one-way ANOVA revealed insignificant difference in age and language age. However, ANOVA revealed that there was a significant difference in social age, the VSMS, SON, spatial tests, memory, concrete reasoning and abstract reasoning.

Whole and local surface area morphometry and cortical volume in Williams syndrome relative to healthy controls

1 Table 2 and Fig. 1 compare SA and CV. Analyses revealed a between-group significant decrease in SA in WS (Fig. 1, Table 2).
2 Figure 2e shows a linear regression analysis, which revealed significant positive correlation between CV and SA bilaterally. This is in accordance with the assumption that CV is the product of SA and Cth (Panizzon *et al.* 2009).

Whole and lobar hemisphere cortical thickness morphology in Williams syndrome relative to healthy controls

1 Table 3 shows no statistical significant differences between children with WS as compared to HC except for the left parietal lobe.
2 Figure 2d depicts regression analyses revealing significant positive correlations between left and right Cth and left and right cortical depth respectively (Fig. 2d). This is particularly in agreement with the principle that the depth map was determined from the fact that the human cerebral cortex is a highly folded sheet with 60–70% of its thickness

Table 2 Summary of differences between Williams syndrome (WS) and healthy controls (HC) in whole hemisphere and each cerebral lobe cortical surface area (CSA in mm^2) and cortical volumes (CV in mm^3) by hemisphere

	Whole hemisphere		Frontal lobe		Temporal lobe		Parietal lobe		Occipital lobe	
	CSA	CV	CSA	CV	CSA	CV	CSA	CV	CSA	CV
Left hemisphere										
WS	73600.23 ± 7658.39	205368.50 ± 26837.01	28286.15 ± 2202.74	83203.04 ± 8863.67	17460.28 ± 2142.34	50330.92 ± 6818.00	17224.45 ± 2740.09	45783.05 ± 8850.99	10608.34 ± 1633.85	25851.48 ± 4788.42
HC	95455.42 ± 7026.59	254831.13 ± 20551.48	36612.58 ± 3949.57	105410.26 ± 9290.75	21928.80 ± 1938.49	61463.63 ± 4941.53	24100.74 ± 1335.41	58625.39 ± 6206.55	12741.30 ± 1785.96	29430.75 ± 4761.36
t statistic	6.65	4.63	5.82	5.47	4.89	4.18	7.13	3.76	2.80	
(*P*-value)	(0.001)	(0.01)	(0.01)	(0.01)	(0.02)	(0.02)	(0.001)	(0.02)	(0.05)	n.s
Right hemisphere										
WS	61644.45 ± 27980.72	209044.20 ± 19479.97	29745.73 ± 3598.16	86694.22 ± 13214.49	17907.82 ± 2043.80	52361.06 ± 7974.04	16003.76 ± 2138.30	43063.76 ± 5553.84	10764.37 ± 1636.11	26725.15 ± 5218.63
HC	95842.90 ± 6819.66	255717.76 ± 19479.98	37527.68 ± 4293.04	107426.80 ± 9639.17	21846.48 ± 1699.89	60652.63 ± 6143.45	22518.69 ± 1639.12	56078.28 ± 5336.18	13860.05 ± 1119.70	31659.03 ± 2908.67
t statistic	3.76	4.25	4.39	4.01	4.69	2.61	7.65	5.34	4.94	2.62
(*P*-value)	(0.04)	(0.02)	(0.02)	(0.02)	(0.01)	(0.05)	(0.001)	(0.01)	(0.01)	(0.05)

n.s, not significant.

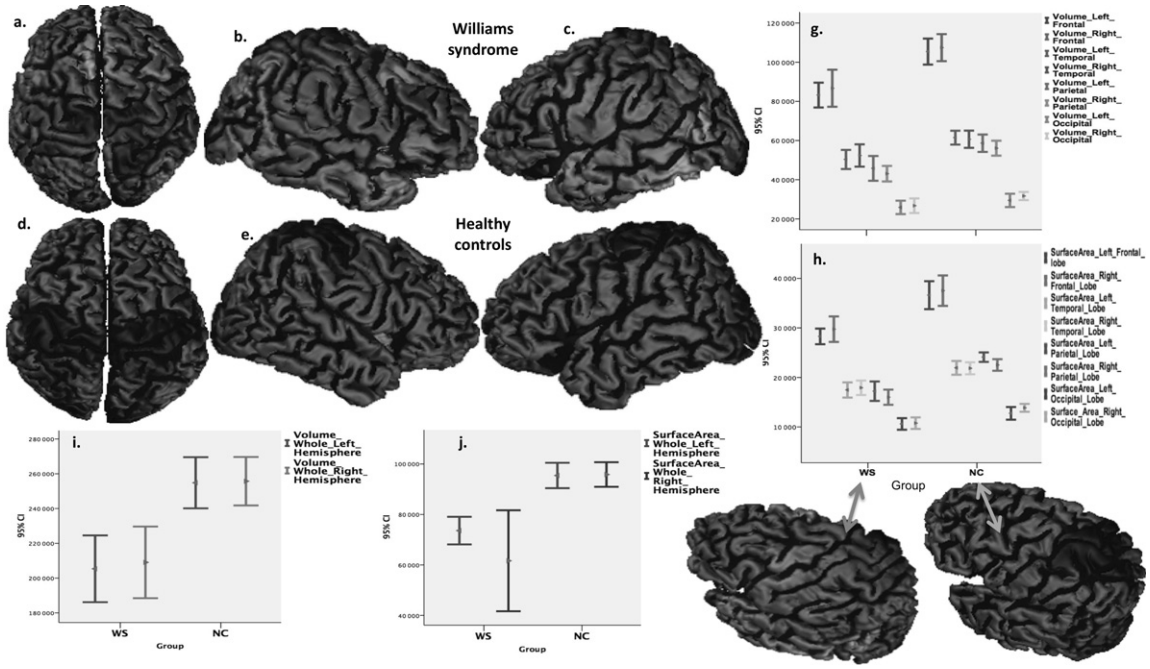

Figure 1 An estimated model using the Civet cortical morphology measures and plots of total and lobar surface area and cortical volume depicting decreased surface area and cortical volume in Williams syndrome (WS) patients relative to age matched healthy controls. NC, normal controls.

buried within folds (Zilles *et al.* 1988; Van Essen 1997).

Whole and local gyrification index and cortical complexity in Williams syndrome relative to healthy controls

1 Table 3 and Fig. 2b,c report statistically significant differences between GI whole hemisphere and lobar-specific analyses with a significant increase in GI in WS. Table 3 shows statistically significant differences between CC whole hemisphere and lobar-specific analyses with a significant decrease in CC in WS in the right frontal and the right parietal lobes.

Multiple regression analyses between whole and local brain morphological measures and neuropsychologiocal scores

1 *SON scores*: *Positive* correlations revealed significance between the *volume* of frontal cortex bilaterally left: $r = 0.75$; $r^2 = 0.56$; $F = 25.37$; $P < 0.0001$ and right $r = 0.65$; $r^2 = 0.41$; $F = 14.13$; $P < 0.001$; the bilateral parietal cortices left $r = 0.55$; $r^2 = 0.30$; $F = 8.71$; $P < 0.01$ and right $r = 0.68$; $r^2 = 0.47$; $F = 17.49$; $P < 0.0001$. Interestingly *negative* correlations revealed significance for the relationship between SON scores and *GI* in the occipital cortices bilaterally: left $r = 0.47$; $r^2 = 0.22$; $F = 5.68$; $P < 0.02$, right $r = 42$; $r^2 = 0.18$; $F = 4.25$; $P < 0.05$ and the right parietal cortex $r = 0.47$; $r^2 = 0.22$; $F = 5.57$; $P < 0.02$. Regarding *SA* significant results were noted in the frontal cortices left $r = 0.69$; $r^2 = 0.47$; $F = 17.91$; $P < 0.0001$ and right $r = 0.61$; $r^2 = 0.38$; $F = 12.10$; $P < 0.002$, parietal cortices left $r = 0.63$; $r^2 = 0.40$; $F = 13.17$; $P < 0.002$ and right $r = 0.73$; $r^2 = 0.53$; $F = 22.82$; $P < 0.0001$, and the occipital cortices left $r = 0.45$; $r^2 = 0.21$; $F = 5.20$; $P < 0.03$ and right $r = 0.54$; $r^2 = 0.29$; $F = 8.23$; $P < 0.01$ (Fig. 3).

2 *Social IQscores*: Contrary to the SON IQ, which mainly showed a positive association with frontal, parietal and occipital CV, SA and a negative association with GI, social IQ as assessed by the VSMS revealed significant positive association with the SA of frontal cortices left $r = 0.60$; $r^2 = 0.36$; $F = 11.39$; $P < 0.003$, right $r = 0.52$; $r^2 = 0.27$; $F = 7.30$; $P < 0.01$ and temporal cortices left $r = 0.55$;

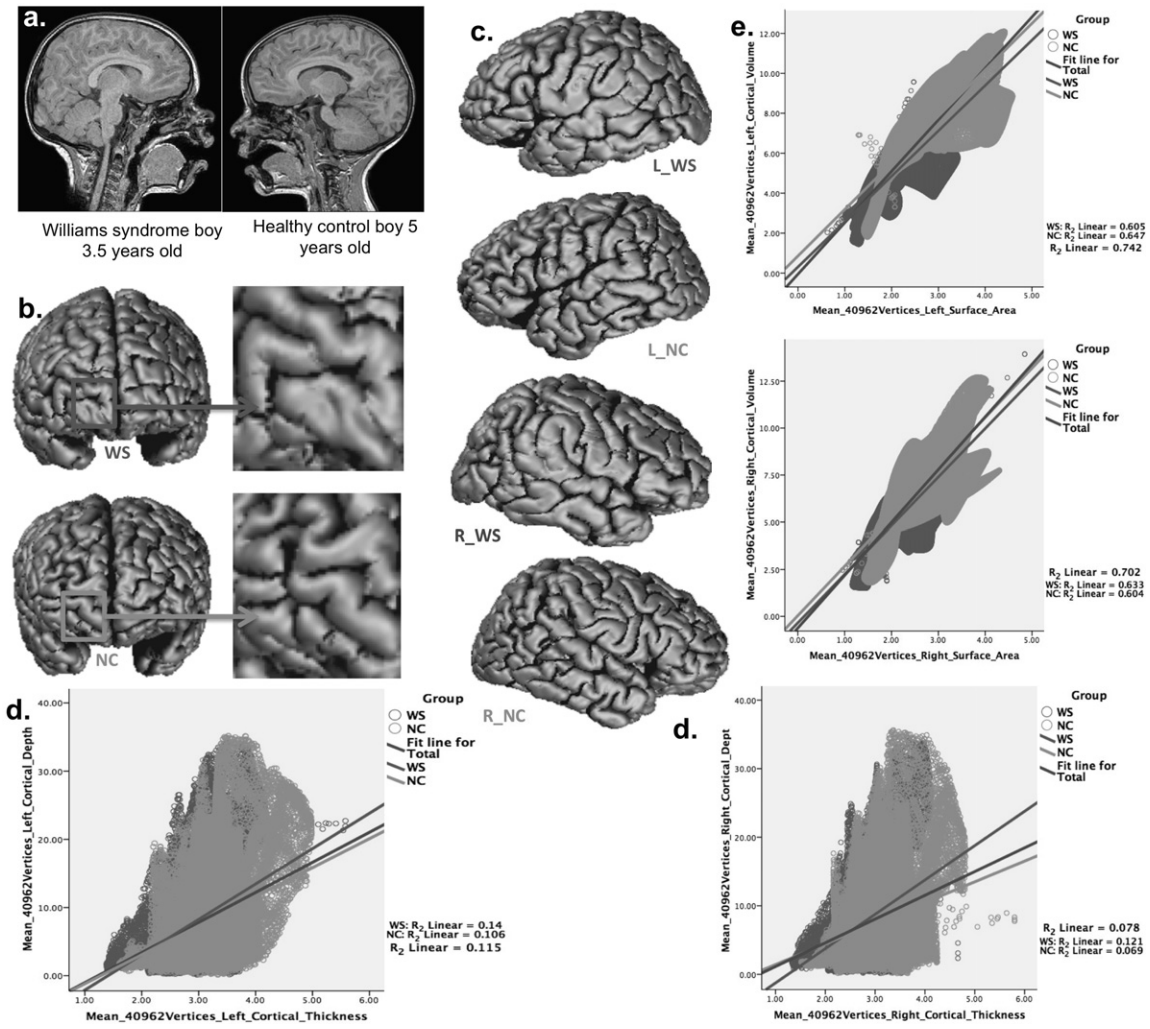

Figure 2 An estimated model using the Civet cortical morphology measures of gyrification (b and c) in children with Williams syndrome (WS) compared to healthy controls (a). Multiple regression plots of cortical morphology vertices in Fig. 2d,e depicting the relationship between on the one hand cortical thickness and cortical depth, and on the other hand surface area and cortical volume. Specifically please note that Fig. 2e shows a linear regression analysis, which revealed significant positive correlation between cortical volume and surface area bilaterally. This is in accordance with the assumption that cortical volume is the product of surface area and cortical thickness (Panizzon *et al.* 2009). On the other hand, Fig. 2d is particularly in agreement with the principle that the depth map was determined from the fact that the human cerebral cortex is a highly folded sheet with 60–70% of its thickness buried within folds (Zilles *et al.* 1988; Van Essen 1997). NC, normal controls.

$r^2 = 0.30$; $F = 8.56$; $P < 0.01$ and right $r = 0.48$; $r^2 = 0.23$; $F = 5.94$; $P < 0.02$ (Fig. 3).

Discussion

We applied the most comprehensive fully automated surface-based morphometry to assemble the pieces of the cortical morphology puzzle in WS, which is caused by haploinsufficiency of multiple genes involved in brain neuronal migration, maturation and the consequent cortical laminar organisation. Our findings demonstrate (1) insignificant whole bilateral hemispheric Cth between WS and HC except for the left parietal lobe; (2) whole hemispheric and lobar significant decrease in SA and CV in WS; (3) local frontal and parietal

Table 3 Summary of differences between Williams syndrome (WS) and healthy controls (HC) in whole hemisphere and each cerebral lobe cortical thickness (Cth), gyrification index (GI) and cortical complexity (CC) by hemisphere in mm

	Whole hemisphere			Frontal lobe			Temporal lobe			Parietal lobe			Occipital lobe		
	Cth	GI	CC	Cth	CSA	CC	Cth	GI	CC	Cth	GI	CC	Cth	GI	CC
Left hemisphere															
WS	3.51 ± 0.18	3.21 ± 0.36	2.23 ± 0.007	3.67 ± 0.22	3.39 ± 0.51	2.22 ± 0.008	3.57 ± 0.16	3.19 ± 0.33	2.24 ± 0.009	3.43 ± 0.15	3.61 ± 0.48	2.25 ± 0.013	3.15 ± 0.21	2.50 ± 0.24	2.24 ± 0.012
HC	3.44 ± 0.16	2.78 ± 0.15	2.24 ± 0.004	3.65 ± 0.19	2.80 ± 0.15	2.22 ± 0.007	3.49 ± 0.21	2.85 ± 0.19	2.27 ± 0.010	3.25 ± 0.15	3.11 ± 0.19	2.26 ± 0.011	3.12 ± 0.15	2.20 ± 0.15	2.24 ± 0.013
t statistic	3.14	2.98	2.60	2.76	3.74										
(*P*-value)	n.s	(0.04)	n.s	n.s	(0.05)	(0.71)	0.38	(0.05)	n.s	0.04	(0.05)	n.s	n.s	(0.04)	n.s
Right hemisphere															
WS	3.52 ± 0.19	3.23 ± 0.30	2.24 ± 0.006	3.63 ± 0.21	3.31 ± 0.38	2.22 ± 0.004	3.59 ± 0.18	3.21 ± 0.28	2.26 ± 0.007	3.44 ± 0.23	3.69 ± 0.46	2.26 ± 0.009	3.21 ± 0.20	2.62 ± 0.26	2.25 ± 0.014
HC	3.41 ± 0.16	2.76 ± 0.12	2.24 ± 0.003	3.61 ± 0.18	2.78 ± 0.14	2.23 ± 0.005	3.42 ± 0.23	2.73 ± 0.17	2.25 ± 0.008	3.26 ± 0.15	3.19 ± 0.13	2.27 ± 0.009	3.10 ± 0.16	2.27 ± 0.10	2.25 ± 0.009
t statistic	4.10	3.51	2.60	3.79	3.35	2.31	4.10								
(*P*-value)	n.s	(0.03)	n.s	n.s	(0.04)	(0.05)	n.s	(0.04)	n.s	n.s	(0.05)	(0.05)	n.s	(0.03)	n.s

n.s, not significant.

decrease in CC; (4) a whole hemispheric and lobar significant increase in GI in WS; and (5) an association between the behavioural phenotypes (*memory, abstract and concrete reasoning, especially visuospatial ability deficits*) and brain morphology. These findings provide further *in vivo* 3D maps magnetic resonance imaging evidence to the Galaburda and colleagues findings demonstrating several cytoarchitectonical anomalies, which included a *reduction in columnar organisation* throughout the cortex, abnormal neuronal orientation and a generalised increase in cell packing density (Galaburda *et al.* 1994). In the following sections we will further discuss the present findings in light of other neuroimaging studies and the Rakic radial-unit hypothesis of cortical development (Rakic 1995).

The relatively preserved Cth in the frontal and temporal lobes are in accordance with Jernigan and colleagues (Jernigan *et al.* 1993) who concluded that frontal and temporal limbic structures are relatively preserved in WS. In addition, Cth preservation of these two brain structures is in agreement with the WS behavioural phenotype presented with relatively preserved language, social, emotional, memory and auditory functions (Udwin & Yule 1991; Gosch *et al.* 1994; Morris & Mervis 2000; Reiss *et al.* 2000; Schmitt *et al.* 2001; Holinger *et al.* 2005). We should note that the frontal and temporal Cth was slightly increased in WS, however it did not reach significant statistical difference as in the Thompson and colleagues study (Thompson *et al.* 2005). This may be due to the age difference between the two studies: here the range is 2.27 to 14.6 compared to 12–50 years of age in the Thompson's study. The sole main effect in the left parietal lobe Cth difference between WS and HC accord with the WS visuospatial construction deficit and its associated decrease in grey matter concentration in the left parieto-occipital region, known to be specifically involved in visuospatial information constructs (Wang *et al.* 1995; Atkinson 1997; Klein & Mervis 1999; Meyer-Lindenberg *et al.* 2004; Boddaert *et al.* 2006). Interestingly, a negative correlation revealed significance between GI in the left occipital and right parietal lobes and the SON IQ scores (Fig. 3), which is in agreement with the visuospatial construction deficit seen in WS children. However, here there was no significant difference in the occipital lobe between WS and HC in Cth. This

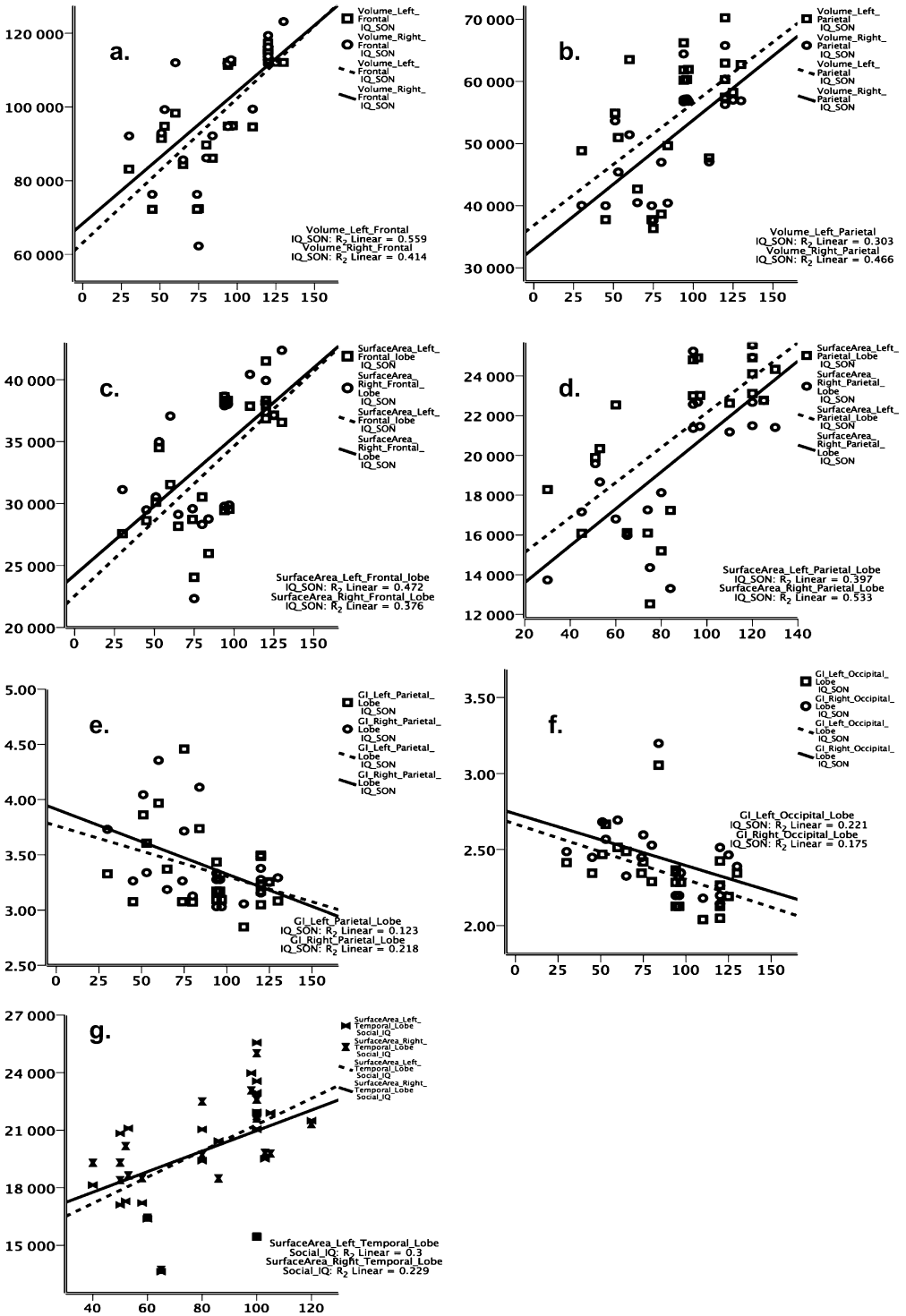

Figure 3 Multiple regression scatter plots showing the correlation between neuropsychological assessments and brain morphological measures: (a) positive correlation between the Snijders-Oomen Nonverbal Intelligence (SON) Tests and cortical volume of the frontal cortex bilaterally, which is in agreement with the role of the frontal cortices in concrete reasoning and memory tests; (b) shows a positive correlation with the parietal cortices bilaterally which is in agreement with their role in abstract reasoning. The same applies for surface area in (c) (frontal) and (d) (parietal). However, (e) and (f) depicts a negative correlation between gyrification index of the left and right parietal and occipital cortices respectively and the SON scores, which is in good agreement with their role in visuospatial construction and the deficits seen in Williams syndrome. On the other hand, g. shows positive correlation between the social intelligence quotient as measured by the Vineland Social Maturity Scale and the surface area in the temporal cortices bilaterally, which is in agreement with the role the temporal cortex plays in social intelligence.

finding is in agreement with previous reports demonstrating that the difficulty for individuals with WS appears to involve visuospatial construction *per se*, rather than visual perception in general (King *et al.* 1997).

On one hand, the reduction in SA, CV and CC is in agreement with the reduction in columnar organisation findings through quantitative cytoarchitectonics (Galaburda *et al.* 1994). In this vein, it has been demonstrated that WS is one of the neurodevelopmental disorders affecting neuronal proliferation and migration, in which disturbances in laminar organisation and neuronal number typically occur (Kaufmann & Moser 2000). Interestingly as is shown in Fig. 3, there is a strong association between SA and WS behavioural phenotypes, that is, SON and social IQ scores. On the other hand, regarding the increase in GI we advance that it may represent an increased amount of deep folds and sulci. As discussed in the introduction, genes on the 7q11.23 region are indeed involved during the critical period when cortical folding occurs, and hence may be related to the increased gyrification. Along these lines, GI is influenced by the underlying cytoarchitecture of the cortex (Rademacher *et al.* 1993; Roland & Zilles 1994) and its neural connectivity (Goldman-Rakic 1981). Several theories implicate factors intrinsic to the cortex in the primary mechanism of folding. For example, it was proposed that greater expansion of outer versus inner cortical layers causes gyrification (Richman *et al.* 1975). Another theory suggests that cortical folding results from the development of intracortical connections (Rakic 1988). These two theories are beyond the scope of the present paper, however, what is of particular relevance here is the *time* of cortical morphogenesis, which could affect the brain lobes differently depending on the time of formation, hence resulting in the relative *increase* and *decrease* in cortical brain regions. In this context, the relatively preserved cortical brain regions (i.e. frontal/parietal/temporal Sylvian fissure) concord with the same time of morphogenesis, which start formation around 14 weeks, superior temporal gyrus 23 weeks, middle temporal sulcus and gyrus 26 weeks, inferior temporal sulcus and gyrus 30 weeks. Interestingly, these brain regions are also associated with a relatively preserved behavioural phenotype (i.e. language and social cognition). Interestingly, however, the deficient behavioural phenotype in WS (i.e. visuospatial construction) has been linked to different brain regions, which start morphogenesis at a different time, for example, the parieto-occipital fissure at 16 weeks, angular gyrus 28 weeks (Chi & Dooling 1976). Worth noting, increased GI is also in agreement with previous reports (Schmitt *et al.* 2002; Gaser *et al.* 2006).

Study novelty and potential confounds

To the best of our knowledge this is the first study to investigate cortical morphology in young children with WS. However, the authors acknowledge several limitations: study sample is relatively small; however, we should emphasise that we used a completely automated method, which has been used by numerous other researchers to assess brain morphology (Charil *et al.* 2003; Hulshoff Pol *et al.* 2004, 2006; Tisserand *et al.* 2004; Chung *et al.* 2005; de Bruin *et al.* 2005; Evans 2006; Giedd *et al.* 2007; Hyde *et al.* 2007; Peper *et al.* 2008; Bermudez *et al.* 2009; Lenroot *et al.* 2009; Schmitt *et al.* 2009; Shaw *et al.* 2009). An advantage of an automated method is that rater error is not a factor. Another important point is the age difference: the younger subject in WS is 2.27, and in HC it is 5.00 years old, yet the between group ANOVA analysis revealed no signifi-

cance because the mean age was ~8 years. Notwithstanding this insignificant statistical difference the present findings should be replicated using an HC as early as 2.27 years old. It is also important to note that regarding gyrification morphogenesis, gyral formation begins around 16 weeks in utero, and most cortical folding is principally defined in the late second and third trimesters of fetal life (Armstrong *et al.* 1995), then the degree of cortical folding to be invariant after the age of 2 years. At this point, we should emphasise that we used a strict registration to a paediatric template method. Kindly note that the fully automated Civet pipeline's third stage after (1) preprocessing the native files and (2) the 'non-uniformity correction' stages, is (3) the 'registration' stages: registration is the process of the alignment of medical image data. In brain-imaging studies, there is a need to put all image volumes into the same spatial coordinate system (stereotaxic space), by aligning all the images to a pre-defined atlas or template brain. This provides a way to compare data from similar locations in different brains and allows quantitative analysis. By default, Civet uses the template generated from 152 subjects in the International Consortium on Brain Imaging project, which is the template often used to bring images into what is referred to as MNI-Talairach stereotaxic space. However, the target model may optionally be changed. Using MNI_AutoReg, these stages will perform a nine-parameter, linear registration to the registration target model in order to later bring native images into MNI-Talairach space. These stages compute the 'transformation' necessary for this. When working with paediatric data, an intermediate step can be added: registration first to a paediatric model, then the output will be registered to the usual target model. This tends to improve the quality of paediatric linear registration. These stages will also handle multispectral data: once T1 images have been registered, T2 and PD weighted images will then be registered linearly to the T1 image. Recently, we have added the ability to perform six- and seven-parameter linear registration. Then the 16th stage of the Civet pipeline is the 'non-linear surface registration' stages: once the cortical surfaces are produced, they need to be aligned with the surfaces of other brains in the data set so Cth data could be compared across participants. To achieve this, *Surfreg* performs a non-linear registration of the surfaces to a pre-defined template surface. This transform is then applied (by resampling) in native space. Note that while the vertices have been aligned, the topological measurements associated with them (e.g. thickness), remain unchanged in this process. Worth noting, we employed surface-based lobe measures for cortical folding pattern by mean of GI and complexity. Because these 3D measures were independent of the imaging plane, we avoided a shortcoming of previous GI measures related to the length of an inner and outer cortical contour in 2D slices of the brain (Zilles *et al.* 1988). Even though both complexity and GI are dependent upon a comparison between the whole area of cerebral cortex and the size of folded area, it is difficult to deduce a mathematical relation between those measures. The GI metric makes use of location-specific information without referring to variable spatial scales, whereas the calculation of complexity considers the surface to be smoothed at a series of different spatial scales (Kiselev *et al.* 2003).

Conclusion

Our data provide novel insights into the neuropsychopathological phenotype of WS early in development. Indeed, a better understanding of the neuropsychopathological phenotype in children with WS may help shed the light on designing more specific therapeutic interventions that will lead to a better quality of life to the patients and their families. Most importantly, the present study may be the basis for further studies exploring the influences of genetics (early in development) and environmental factors (during adulthood) on developmental trajectories in WS. In summary, the early neurodevelopmental effects of a deletion of the WS chromosome 7q11.23 region, spanning 1.5 million to 1.8 million base pairs and containing 26 to 28 genes, allow phenotypes of interest such as Cth, SA, CV, GI and CC to be examined early in development (the youngest WS patients is 2.27 years old) using fully automated magnetic resonance imaging analyses. At this point it is important to emphasise that we are not solely suggesting that direct effects of the WS genes deletions are the sole determinants of the

neurobiological phenotype. Brain development in WS may be shaped by the postnatal environment, which can also shape brain development in their own right by impacting on experience-dependent neuronal plasticity. In essence, our findings indicate that WS is associated with a relatively spared Cth with marked decrease in SA and increase in GI. We speculate that WS is associated with alterations in the mechanistically distinct pathways that shape SA/GI (e.g. cell-cycle dynamics of neural progenitor cell pool) and Cth (e.g. dendritic arborisation/pruning). In this context, to gain a better understanding of the relationship between genetic variation, brain and behaviour in WS, we will need to study these influences longitudinally in a larger sample.

Acknowledgements

We would like to thank the individuals and families who participated in this study. We deeply acknowledge Dr Alan Evans who offered the Egyptian Neuroimaging Neurodevelopmental Genetics Initiative Network to use the McConnell Brain Imaging Centre MNI facilities to analyse the present study data. This study is supported in part by the Faculty of Social Sciences and Politics University of Lausanne, Switzerland. Authors declare no conflict of interest.

References

American Academy of Pediatrics (2001) Health care supervision for children with Williams syndrome. *Pediatrics* **107,** 1192–204.

Armstrong E., Schleicher A., Omran H., Curtis M. & Zilles K. (1995) The ontogeny of human gyrification. *Cereb Cortex* **5,** 56–63.

Atkinson J. (1997) Neural basis of disordered visuo-spatial function in Williams syndrome. *Perception* **26,** 762–762.

Bermudez P., Lerch J. P., Evans A. C. & Zatorre R. J. (2009) Neuroanatomical correlates of musicianship as revealed by cortical thickness and voxel-based morphometry. *Cereb Cortex* **19,** 1583–96. doi: bhn196 [pii]. 10.1093/cercor/bhn196.

Boddaert N., Mochel F., Meresse I., Seidenwurm D., Cachia A. & Brunelle F. (2006) Parieto-occipital grey matter abnormalities in children with Williams syndrome. *NeuroImage* **30,** 721–5. doi: Doi 10.1016/J.Neuroimage.2005.10.051.

de Bruin E. A., Hulshoff Pol H. E., Schnack H. G., Janssen J., Bijl S. & Evans A. C. (2005) Focal brain matter differences associated with lifetime alcohol intake and visual attention in male but not in female non-alcohol-dependent drinkers. *NeuroImage* **26,** 536–45. doi: S1053-8119(05)00080-7 [pii]. 10.1016/j.neuroimage.2005.01.036.

Charil A., Zijdenbos A. P., Taylor J., Boelman C., Worsley K. J. & Evans A. C. (2003) Statistical mapping analysis of lesion location and neurological disability in multiple sclerosis: application to 452 patient data sets. *NeuroImage* **19,** 532–44. doi: S1053811903001174 [pii].

Cherniske E. M., Carpenter T. O., Klaiman C., Young E., Bregman J. & Insogna K. (2004) Multisystem study of 20 older adults with Williams syndrome. *American Journal of Medical Genetics. Part A* **131,** 255–64. doi: 10.1002/ajmg.a.30400.

Chi J. G. & Dooling E. C. (1976) Gyral development of the human brain. *Transactions of the American Neurological Association* **101,** 89–90.

Chung M. K., Robbins S. M., Dalton K. M., Davidson R. J., Alexander A. L. & Evans A. C. (2005) Cortical thickness analysis in autism with heat kernel smoothing. *NeuroImage* **25,** 1256–65. doi: S1053-8119(04)00754-2 [pii]. 10.1016/j.neuroimage.2004.12.052.

Collins D. L., Neelin P., Peters T. M. & Evans A. C. (1994) Automatic 3D intersubject registration of MR volumetric data in standardized Talairach space. *Journal of Computer Assisted Tomography* **18,** 192–205.

Collins D. L., Holmes C. J., Peters T. M. & Evans A. C. (1995) Automatic 3-D model-based neuroanatomical segmentation. *Human Brain Mapping* **3,** 190–208.

Evans A. C. (2006) The NIH MRI study of normal brain development. *NeuroImage* **30,** 184–202. doi: S1053-8119(05)00710-X [pii]. 10.1016/j.neuroimage.2005.09.068.

Ewart A. K., Morris C. A., Atkinson D., Jin W., Sternes K. & Spallone P. (1993) Hemizygosity at the elastin locus in a developmental disorder, Williams syndrome. *Nature Genetics* **5,** 11–16.

Frangiskakis J. M., Ewart A. K., Morris C. A., Mervis C. B., Bertrand J. & Robinson B. F. (1996) LIM-kinase1 hemizygosity implicated in impaired visuospatial constructive cognition. *Cell* **86,** 59–69. doi: S0092-8674(00)80077-X [pii].

Galaburda A. M., Wang P. P., Bellugi U. & Rossen M. (1994) Cytoarchitectonic anomalies in a genetically based disorder: Williams syndrome. *Neuroreport* **5,** 753–7.

Galaburda A. M., Schmitt J. E., Atlas S. W., Eliez S., Bellugi U. & Reiss A. L. (2001) Dorsal forebrain anomaly in Williams syndrome. *Archives of Neurology* **58,** 1865–9.

Gaser C., Luders E., Thompson P. M., Lee A. D., Dutton R. A. & Geaga J. A. (2006) Increased local gyrification

mapped in Williams syndrome. *NeuroImage* **33,** 46–54. doi: S1053-8119(06)00668-9 [pii]. 10.1016/j.neuroimage.2006.06.018.

Genovese C. R., Lazar N. A. & Nichols T. (2002) Thresholding of statistical maps in functional neuroimaging using the false discovery rate. *NeuroImage* **15,** 870–8.

Giedd J. N., Clasen L. S., Wallace G. L., Lenroot R. K., Lerch J. P. & Wells E. M. (2007) XXY (Klinefelter syndrome): a pediatric quantitative brain magnetic resonance imaging case-control study. *Pediatrics* **119,** e232–40. doi: 119/1/e232 [pii]. 10.1542/peds.2005-2969.

Goldman-Rakic P. S. (1981) Prenatal formation of cortical input and development of cytoarchitectonic compartments in the neostriatum of the rhesus monkey. *Journal of Neuroscience* **1,** 721–35.

Gosch A. & Pankau R. (1997) Personality characteristics and behaviour problems in individuals of different ages with Williams syndrome. *Developmental Medicine and Child Neurology* **39,** 527–33.

Gosch A., Stading G. & Pankau R. (1994) Linguistic Abilities in Children with Williams-Beuren Syndrome. *American Journal of Medical Genetics* **52,** 291–6.

Harris S. H. (1982) An evaluation of the Snijders-Oomen Nonverbal Intelligence Scale for Young Children. *Journal of Pediatric Psychology* **7,** 239–51.

Holinger D. P., Bellugi U., Mills D. L., Korenberg J. R., Reiss A. L. & Sherman G. F. (2005) Relative sparing of primary auditory cortex in Williams syndrome. *Brain Research* **1037,** 35–42. doi: S0006-8993(04)01837-2 [pii]. 10.1016/j.brainres.2004.11.038.

Hoogenraad C. C., Koekkoek B., Akhmanova A., Krugers H., Dortland B. & Miedema M. (2002) Targeted mutation of Cyln2 in the Williams syndrome critical region links CLIP-115 haploinsufficiency to neurodevelopmental abnormalities in mice. *Nature Genetics* **32,** 116–27. doi: 10.1038/ng954. ng954 [pii].

Hulshoff Pol H. E., Schnack H. G., Mandl R. C., Cahn W., Collins D. L. & Evans A. C. (2004) Focal white matter density changes in schizophrenia: reduced inter-hemispheric connectivity. *NeuroImage* **21,** 27–35. doi: S105381190300572X [pii].

Hulshoff Pol H. E., Schnack H. G., Posthuma D., Mandl R. C., Baare W. F. & van Oel C. (2006) Genetic contributions to human brain morphology and intelligence. *Journal of Neuroscience* **26,** 10235–42. doi: 26/40/10235 [pii]. 10.1523/JNEUROSCI.1312-06.2006.

Hyde K. L., Lerch J. P., Zatorre R. J., Griffiths T. D., Evans A. C. & Peretz I. (2007) Cortical thickness in congenital amusia: when less is better than more. *Journal of Neuroscience* **27,** 13028–32. doi: 27/47/13028 [pii]. 10.1523/JNEUROSCI.3039-07.2007.

Im K., Lee J. M., Lyttelton O., Kim S. H., Evans A. C. & Kim S. I. (2008a) Brain size and cortical structure in the adult human brain. *Cereb Cortex* **18,** 2181–91. doi: bhm244 [pii]. 10.1093/cercor/bhm244.

Im K., Lee J. M., Won Seo S., Hyung Kim S., Kim S. I. & Na D. L. (2008b) Sulcal morphology changes and their relationship with cortical thickness and gyral white matter volume in mild cognitive impairment and Alzheimer's disease. *NeuroImage* **43,** 103–13. doi: S1053-8119(08)00833-1 [pii]. 10.1016/j.neuroimage.2008.07.016.

Im K., Jo H. J., Mangin J. F., Evans A. C., Kim S. I. & Lee J. M. (2010) Spatial distribution of deep sulcal landmarks and hemispherical asymmetry on the cortical surface. *Cereb Cortex* **20,** 602–11. doi: bhp127 [pii]. 10.1093/cercor/bhp127.

Jernigan T. L., Bellugi U., Sowell E., Doherty S. & Hesselink J. R. (1993) Cerebral morphologic distinctions between Williams and Down syndromes. *Archives of Neurology* **50,** 186–91.

Kaufmann W. E. & Moser H. W. (2000) Dendritic anomalies in disorders associated with mental retardation. *Cereb Cortex* **10,** 981–91.

Kim J. S., Singh V., Lee J. K., Lerch J., Ad-Dab'bagh Y. & MacDonald D. (2005) Automated 3-D extraction and evaluation of the inner and outer cortical surfaces using a Laplacian map and partial volume effect classification. *NeuroImage* **27,** 210–21. doi: S1053-8119(05)00223-5 [pii]. 10.1016/j.neuroimage.2005.03.036.

King J., Atkinson J., Braddick O., Hartley T., Nokes L. & Braddick F. (1997) Dissociation of visually guided action from visual judgment in Williams syndrome children. *Perception* **26,** 762–3.

Kippenhan J. S., Olsen R. K., Mervis C. B., Morris C. A., Kohn P. & Meyer-Lindenberg A. (2005) Genetic contributions to human gyrification: sulcal morphometry in Williams syndrome. *Journal of Neuroscience* **25,** 7840–6. doi: 25/34/7840 [pii]. 10.1523/JNEUROSCI.1722-05.2005.

Kiselev V. G., Hahn K. R. & Auer D. P. (2003) Is the brain cortex a fractal? *NeuroImage* **20,** 1765–74. doi: S105381190300380X [pii].

Klein B. P. & Mervis C. B. (1999) Contrasting patterns of cognitive abilities of 9-and 10-year-olds with Williams syndrome or Down syndrome. *Developmental Neuropsychology* **16,** 177–96.

Lee J. K., Lee J. M., Kim J. S., Kim I. Y., Evans A. C. & Kim S. I. (2006) A novel quantitative cross-validation of different cortical surface reconstruction algorithms using MRI phantom. *NeuroImage* **31,** 572–84. doi: S1053-8119(06)00007-3 [pii]. 10.1016/j.neuroimage.2005.12.044.

Lenhoff H. M., Perales O. & Hickok G. (2001) Absolute pitch in Williams syndrome. *Music Perception* **18,** 491–503.

Lenroot R. K., Schmitt J. E., Ordaz S. J., Wallace G. L., Neale M. C. & Lerch J. P. (2009) Differences in genetic and environmental influences on the human cerebral

cortex associated with development during childhood and adolescence. *Human Brain Mapping* **30,** 163–74. doi: 10.1002/hbm.20494.

Lerch J. P. & Evans A. C. (2005) Cortical thickness analysis examined through power analysis and a population simulation. *NeuroImage* **24,** 163–73. doi: S1053-8119(04)00418-5 [pii]. 10.1016/j.neuroimage.2004.07.045.

Luders E., Narr K. L., Thompson P. M., Rex D. E., Jancke L. & Toga A. W. (2006a) Hemispheric asymmetries in cortical thickness. *Cereb Cortex* **16,** 1232–8. doi: bhj064 [pii]. 10.1093/cercor/bhj064.

Luders E., Thompson P. M., Narr K. L., Toga A. W., Jancke L. & Gaser C. (2006b) A curvature-based approach to estimate local gyrification on the cortical surface. *NeuroImage* **29,** 1224–30. doi: S1053-8119(05)00654-3 [pii]. 10.1016/j.neuroimage.2005.08.049.

Lyttelton O., Boucher M., Robbins S. & Evans A. (2007) An unbiased iterative group registration template for cortical surface analysis. *NeuroImage* **34,** 1535–44. doi: S1053-8119(06)01033-0 [pii]. 10.1016/j.neuroimage.2006.10.041.

Lyttelton O. C., Karama S., Ad-Dab'bagh Y., Zatorre R. J., Carbonell F. & Worsley K. (2009) Positional and surface area asymmetry of the human cerebral cortex. *NeuroImage* **46,** 895–903. doi: S1053-8119(09)00326-7 [pii]. 10.1016/j.neuroimage.2009.03.063.

Manni F., Leonardi P., Barakat A., Rouba H., Heyer E. & Klintschar M. (2002) Y-chromosome analysis in Egypt suggests a genetic regional continuity in Northeastern Africa. *Human Biology* **74,** 645–58.

Marenco S., Siuta M. A., Kippenhan J. S., Grodofsky S., Chang W. L. & Kohn P. (2007) Genetic contributions to white matter architecture revealed by diffusion tensor imaging in Williams syndrome. *Proceedings of the National Academy of Sciences of the United States of America* **104,** 15117–22.

Meng X., Lu X., Li Z., Green E. D., Massa H. & Trask B. J. (1998) Complete physical map of the common deletion region in Williams syndrome and identification and characterization of three novel genes. *Human Genetics* **103,** 590–9.

Meyer-Lindenberg A., Kohn P., Mervis C. B., Kippenhan J. S., Olsen R. K. & Morris C. A. (2004) Neural basis of genetically determined visuospatial construction deficit in Williams syndrome. *Neuron* **43,** 623–31. doi: 10.1016/j.neuron.2004.08.014. S0896627304005215 [pii].

Moore C., O'Keefe S. L., Lawhon D. & Tellegen P. (1998) Concurrent validity of the Snijders-Oomen Nonverbal Intelligence Test 2 1/2-7-Revised with the Wechsler Preschool and Primary Scale of Intelligence – Revised. *Psychological Reports* **82,** 619–25.

Morris C. A. & Mervis C. B. (2000) Williams syndrome and related disorders. *Annual Review of Genomics and Human Genetics* **1,** 461–84. doi: 1/1/461 [pii]. 10.1146/annurev.genom.1.1.461.

Morris C. A., Leonard C. O., Dilts C. & Demsey S. A. (1990) Adults with Williams Syndrome. *American Journal of Medical Genetics* **6,** 102–7.

Panizzon M. S., Fennema-Notestine C., Eyler L. T., Jernigan T. L., Prom-Wormley E. & Neale M. (2009) Distinct genetic influences on cortical surface area and cortical thickness. *Cereb Cortex* **19,** 2728–35. doi: bhp026 [pii]. 10.1093/cercor/bhp026.

Peper J. S., Brouwer R. M., Schnack H. G., van Baal G. C., van Leeuwen M. & van den Berg S. M. (2008) Cerebral white matter in early puberty is associated with luteinizing hormone concentrations. *Psychoneuroendocrinology* **33,** 909–15. doi: S0306-4530(08)00079-6 [pii]. 10.1016/j.psyneuen.2008.03.017.

Plissart L., Borghgraef M., Volcke P., Van den Berghe H. & Fryns J. P. (1994) Adults with Williams-Beuren syndrome: evaluation of the medical, psychological and behavioral aspects. *Clinical Genetics* **46,** 161–7.

Pober B. R. (2010) Williams-Beuren syndrome. *The New England Journal of Medicine* **362,** 239–52. doi: 362/3/239 [pii]. 10.1056/NEJMra0903074.

Preus M. (1984) The Williams syndrome: objective definition and diagnosis. *Clinical Genetics* **25,** 422–8.

Rademacher J., Caviness V. S., Jr, Steinmetz H. & Galaburda A. M. (1993) Topographical variation of the human primary cortices: implications for neuroimaging, brain mapping, and neurobiology. *Cereb Cortex* **3,** 313–29.

Rakic P. (1988) Specification of cerebral cortical areas. *Science* **241,** 170–6.

Rakic P. (1995) A small step for the cell, a giant leap for mankind: a hypothesis of neocortical expansion during evolution. *Trends in Neurosciences* **18,** 383–8. doi: 016622369593934P [pii].

Reiss A. L., Eliez S., Schmitt J. E., Straus E., Lai Z. & Jones W. (2000) IV. Neuroanatomy of Williams syndrome: a high-resolution MRI study. *Journal of Cognitive Neuroscience* **12** (Suppl 1), 65–73.

Richman D. P., Stewart R. M., Hutchinson J. W. & Caviness V. S. (1975) Mechanical Model of Brain Convolutional Development. *Science* **189,** 18–21.

Roland P. E. & Zilles K. (1994) Brain atlases–a new research tool. *Trends in Neurosciences* **17,** 458–67.

Ross A. K., Hazlett H. C., Garrett N. T., Wilkerson C. & Piven J. (2005) Moderate sedation for MRI in young children with autism. *Pediatric Radiology* **35,** 867–71. doi: 10.1007/s00247-005-1499-2.

Schmitt J. E., Eliez S., Bellugi U. & Reiss A. L. (2001) Analysis of cerebral shape in Williams syndrome. *Archives of Neurology* **58,** 283–7. doi: noc90068 [pii].

Schmitt J. E., Watts K., Eliez S., Bellugi U., Galaburda A. M. & Reiss A. L. (2002) Increased gyrification in Williams syndrome: evidence using 3D MRI methods. *Developmental Medicine and Child Neurology* **44,** 292–5.

Schmitt J. E., Lenroot R. K., Ordaz S. E., Wallace G. L., Lerch J. P. & Evans A. C. (2009) Variance decomposition of MRI-based covariance maps using genetically informative samples and structural equation modeling. *NeuroImage* **47,** 56–64. doi: S1053-8119(08)00772-6 [pii]. 10.1016/j.neuroimage.2008.06.039.

Shaw P., Sharp W. S., Morrison M., Eckstrand K., Greenstein D. K. & Clasen L. S. (2009) Psychostimulant treatment and the developing cortex in attention deficit hyperactivity disorder. *The American Journal of Psychiatry* **166,** 58–63. doi: appi.ajp.2008.08050781 [pii]. 10.1176/appi.ajp.2008.08050781.

Sled J. G., Zijdenbos A. P. & Evans A. C. (1998) A nonparametric method for automatic correction of intensity nonuniformity in MRI data. *IEEE Transactions on Medical Imaging* **17,** 87–97. doi: 10.1109/42.668698.

Snijders J. T. & Snijders-Oomen N. (1976) *Snijders-Oomen Non-Verbal Intelligence Scale: S.O.N. 2 1/2-7.* H.D. Tjeenk Willink, Groningen.

Thompson P. M., Lee A. D., Dutton R. A., Geaga J. A., Hayashi K. M. & Eckert M. A. (2005) Abnormal cortical complexity and thickness profiles mapped in Williams syndrome. *Journal of Neuroscience* **25,** 4146–58. doi: 25/16/4146 [pii]. 10.1523/JNEUROSCI.0165-05.2005.

Thompson P. M., Dutton R. A., Hayashi K. M., Lu A., Lee S. E. & Lee J. Y. (2006) 3D mapping of ventricular and corpus callosum abnormalities in HIV/AIDS. *NeuroImage* **31,** 12–23. doi: S1053-8119(05)02516-4 [pii]. 10.1016/j.neuroimage.2005.11.043.

Tisserand D. J., van Boxtel M. P., Pruessner J. C., Hofman P., Evans A. C. & Jolles J. (2004) A voxel-based morphometric study to determine individual differences in gray matter density associated with age and cognitive change over time. *Cereb Cortex* **14,** 966–73. doi: 10.1093/cercor/bhh057. bhh057 [pii].

Tomc S. A., Williamson N. K. & Pauli R. M. (1990) Temperament in Williams syndrome. *American Journal of Medical Genetics* **36,** 345–52.

Udwin O. & Yule W. (1991) A cognitive and behavioral-phenotype in Williams syndrome. *Journal of Clinical and Experimental Neuropsychology* **13,** 232–44.

Van Essen D. C. (1997) A tension-based theory of morphogenesis and compact wiring in the central nervous system. *Nature* **385,** 313–18. doi: 10.1038/385313a0.

Van Essen D. C. (2005) A Population-Average, Landmark- and Surface-based (PALS) atlas of human cerebral cortex. *NeuroImage* **28,** 635–62. doi: Doi 10.1016/J.Neuroimage.2005.06.058.

Wang P. P., Doherty S., Rourke S. B. & Bellugi U. (1995) Unique profile of visuo-perceptual skills in a genetic syndrome. *Brain and Cognition* **29,** 54–65.

Wang Y. K., Samos C. H., Peoples R., Perez-Jurado L. A., Nusse R. & Francke U. (1997) A novel human homologue of the Drosophila frizzled wnt receptor gene binds wingless protein and is in the Williams syndrome deletion at 7q11.23. *Human Molecular Genetics* **6,** 465–72. doi: dda053 [pii].

Wiegand L. C., Warfield S. K., Levitt J. J., Hirayasu Y., Salisbury D. F. & Heckers S. (2005) An in vivo MRI study of prefrontal cortical complexity in first-episode psychosis. *The American Journal of Psychiatry* **162,** 65–70. doi: 162/1/65 [pii]. 10.1176/appi.ajp.162.1.65.

Yoon U., Fonov V. S., Perusse D. & Evans A. C. (2009) The effect of template choice on morphometric analysis of pediatric brain data. *NeuroImage* **45,** 769–77. doi: S1053-8119(08)01306-2 [pii]. 10.1016/j.neuroimage.2008.12.046.

Zijdenbos A. P., Forghani R. & Evans A. C. (2002) Automatic 'pipeline' analysis of 3-D MRI data for clinical trials: application to multiple sclerosis. *IEEE Transactions on Medical Imaging* **21,** 1280–91. doi: 10.1109/TMI.2002.806283.

Zilles K., Armstrong E., Schleicher A. & Kretschmann H. J. (1988) The human pattern of gyrification in the cerebral cortex. *Anatomy and Embryology* **179,** 173–9.

Accepted 25 August 2011